



Published in final edited form as:

*Int Ophthalmol Clin.* 2017 ; 57(3): 75–86. doi:10.1097/IIO.000000000000172.

## BIOMECHANICAL DIAGNOSTICS OF THE CORNEA

Vinicius Silbiger De Stefano, M.D.<sup>1,2</sup> and William J. Dupps Jr., M.D., Ph.D.<sup>1,3</sup>

<sup>1</sup>Cole Eye Institute, Cleveland Clinic, Cleveland, OH, United States

<sup>2</sup>Dept. of Ophthalmology and Visual Sciences, Federal University of Sao Paulo, Sao Paulo, Brazil

<sup>3</sup>Dept. of Biomedical Engineering, Lerner Research Institute, Cleveland Clinic, Cleveland, OH, United States

### Abstract

Biomechanics is the science concerned with the origin and effects of forces that act on living organisms. The cornea is a complex composite whose behavior depends on its structural subcomponents and their organizational motifs. A better understanding of its biomechanical features is essential to understand the consequences of procedures such as excimer laser refractive surgery and corneal collagen crosslinking and to improve the detection and management of ectatic corneal diseases. Devices such as the Ocular Response Analyzer and the Corvis STL use an air-puff to perturb the cornea and assess biomechanical responses. Although both devices use similar approaches, data produced by them cannot be used interchangeably. Moreover, current commercial technologies lack capabilities for regional property discrimination, which is of paramount importance for comprehensive biomechanical analysis. To address this gap, other methodologies such as optical coherence elastography and Brillouin microscopy are being developed and early *in vivo* studies show promising results. Finally, another important tool for studying complex structures is computational modeling using the finite element method. The cornea can be represented as a mesh of smaller geometric elements with specific material properties. Advances in this area have the potential to enhance diagnosis, enable personalized risk assessment, and optimize treatment design toward the goal of improving safety and outcomes for corneal and refractive surgery patients.

### INTRODUCTION

The cornea contains the first cellular surface of the eye's optical system and contributes approximately two-thirds of the optical power of the relaxed eye. As a result, miniscule changes in the cornea's shape induce substantial variations in the image formation process. Corneal diseases such as keratoconus as well as corneal refractive surgery can generate significant changes in the cornea's optical properties. An ongoing challenge is to understand the relationship between the mechanical and structural changes that produce those clinically measured optical modifications in pathological conditions and after refractive surgery and to understand their evolution over time. Better understanding of the biomechanics of the cornea

Correspondence: William J. Dupps, Jr., M.D., Ph.D., Cole Eye Institute, Cleveland Clinic, 9500 Euclid Avenue, i-32, Cleveland, OH 44195. [bjdupps@sbcglobal.net](mailto:bjdupps@sbcglobal.net).

Commercial Relationships Disclosure: VSS – none; WJD – OptoQuest (Patent)

is thus essential to comprehend the consequences of modifications in the geometry of the cornea after excimer laser refractive surgery or non-ablative interventions such as corneal collagen crosslinking (CXL), to improve the diagnosis and management of ectatic corneal disorders such as keratoconus, and to understand the biomechanics of intraocular pressure (IOP).

The cornea is a complex biomechanical composite that responds to stress according to its structural subcomponents and their organization. The stroma and Bowman layer are the chief collagenous layers of the cornea and thus provide the majority of the cornea's tensile strength.<sup>1-3</sup> With regard to microstructure, around 300 collagen lamellae run across the corneal stroma and are stacked with angular offsets; this orientation becomes increasingly random in the anterior stroma, where significantly more oblique branching and interweaving are noted, which are also more extensive in the corneal periphery than in its center.<sup>4</sup> Interweaving of collagen bundles between neighboring lamellae provides a structural mechanism for shear (sliding) resistance, sharing of tensile loads between lamellae, and distribution of stress across the cornea.<sup>5</sup> In addition, X-ray diffraction studies provide evidence that the collagen fibrils are preferentially oriented superior to inferior and nasal to temporal in the central cornea and a predominantly circumferential in the corneal periphery that favors conservation of limbal circumferential dimensions even in ectatic disease.<sup>6</sup>

## GENERAL CONCEPTS OF BIOMECHANICS

Biomechanics is the science concerned with the origin and effects of forces that act within and upon living organisms at the micro- and macroscopic level. The knowledge of biomechanical features of human tissue allows us to understand and predict the alterations in certain structures and organs. This may permit the development of novel strategies for the management, diagnosis, prognosis, and treatment of biomechanically-related pathologies. Other fields in medicine are increasingly applying biomechanical concepts to clinical and surgical procedures, particularly in the areas of cardiovascular science, orthopedics, and rehabilitation.

Assessing the biomechanical response of living tissue is complex and demands knowledge of some basic concepts of mechanical engineering. First among these is the elastic modulus, or Young's modulus, which describes how much a load (IOP) will deform the material (cornea) under specific conditions. The material deformation is expressed as a strain and will lead to an internal response within the material (stress). Young's modulus is depicted by the slope of the stress-strain plot (Figure 1). The greater the slope is, the higher the modulus and the stiffer the material are such that greater force is required to deform a more rigid material.

Another important material property is viscoelasticity, which implies that the material behavior is strain rate (time) dependent and is different during loading and unloading phases. As opposed to the symmetric loading-unloading behavior of purely elastic materials, viscoelastic materials return to their pre-stress configuration via different stress-strain pathways that depend on loading rates. This discordance between loading and unloading behavior can be partially characterized by hysteresis, which represents the amount of energy

dissipated during the loading-unloading process, usually as thermal energy. Viscoelasticity is an intrinsic characteristic of every living tissue.

Therefore, the cornea does not behave as a linearly elastic structure. It is a complex anisotropic composite with nonlinear elastic and viscoelastic properties. It is anisotropic because its properties are not directionally uniform. It behaves as a composite because its properties are determined by the interaction of diverse materials like collagen and a polyanionic, hydrophilic ground substance. Understanding these concepts and how they apply to the cornea and the eye as a whole highlights why it is so difficult to define the cornea biomechanically with a single number or scale. Moreover, the distinct features found when the center is compared to the periphery and when the anterior cornea is compared to the posterior regions makes biomechanical characterization an even more challenging task.

## CLINICAL MEASUREMENTS OF CORNEAL BIOMECHANICS

A common laboratory method to assess corneal biomechanics is extensimetry, in which a strip of tissue is fixed on both ends and pulled apart to establish a relationship between applied force and tissue distension. It has revealed substantial deficits in elastic tensile strength in keratoconus and suggests a diagnostic role for the elastic modulus in the clinical setting.<sup>4,7,8</sup> Nonetheless, the impossibility of performing this test in vivo and the artifact resulting from testing corneal tissue outside of its native curved configuration has prompted accelerated efforts to develop nondestructive, noninvasive tools for clinical biomechanical property measurement.

### Dynamic Bidirectional Applanation

The first commercially available device capable of evaluating the cornea's biomechanical features was the Ocular Response Analyzer (ORA, Reichert, Inc., Depew, NY),<sup>9</sup> which utilizes a high-speed air-puff to quantify the dynamics of corneal deformation and recovery as an indicator of corneal hysteresis (CH). Figure 2 illustrates a typical response waveform. CH is the difference between the ingoing and outgoing applanation pressures ( $P_1 - P_2$ ) and represents the energy loss due to viscous damping in the cornea and extracorneal structures. This difference would be equal to zero in an isotropic material and is always positive in a viscoelastic tissue: as mentioned before, pressure is always greater at the first applanation event ("loading") than the second ("unloading"). A higher CH indicates a greater capacity for absorption and dissipation of kinetic energy in the tissue. Eyes with a higher CH (i.e. greater viscoelastic damping) present a signal analysis which shifts the applanation peaks to the right, resulting in a higher  $P_1$ , a lower  $P_2$ , and an increased CH. The corneal resistance factor (CRF) is derived from the same dual-applanation signal and is proposed to be a measure of the overall elastic resistance of the cornea. The formula for the CRF is similar to CH but incorporates an empirically determined adjustment factor ( $k$ ) to  $P_2$  ( $CRF = P_1 - kP_2$ ). Since  $k = 0.7$  and is less than 1, this weighting towards the first applanation event increases the influence of the loading pressure,  $P_1$ , which emphasizes the role of the initial elastic deformation response, but it fundamentally remains a viscoelastic parameter due to the inclusion of the unloading applanation pressure,  $P_2$ . The ORA also reports two IOP values: the Goldmann-correlated IOP ( $IOP_G$ ) derived from the mean of  $P_1$  and  $P_2$  and the

cornea-compensated IOP (IOP<sub>CC</sub>), where the latter is helpful in assessing IOP with some degree of compensation for atypical corneas.

Though originally designed as a tool for IOP measurement, the ORA has been actively investigated as a tool for characterizing biomechanical abnormalities in keratoconus and ectasia. Both CH and CRF are lower in eyes affected by keratoconus, and they are associated with keratoconus severity, suggesting that viscous damping capacity and overall corneal resistance are reduced in this disease.<sup>9</sup> Nevertheless, the greater clinical challenge of distinguishing between normal and low-grade or forme fruste keratoconus is not resolved by CH or CRF alone, with studies reporting inconsistent discriminatory performance results.<sup>10,11</sup>

Several studies have demonstrated that CH and CRF are not changed after collagen CXL for keratoconus despite the common-held expectation that these indicators of biomechanical state should increase after treatment.<sup>12</sup> In an effort to better understand the device's signal features, investigators and the manufacturer have addressed other characteristics provided by the ORA beyond CH and CRF.<sup>13</sup> The morphology of the infrared signal contains additional information that is not represented by CH or CRF, and significant changes in some waveform-derived variables (or custom variables) are noted after CXL treatment.<sup>14</sup> As an example of such custom variables, hysteresis loop area (HLA) has been shown to be more sensitive for detecting changes after corneal CXL and in distinguishing between normal and keratoconus suspects than some standard variables. By analyzing the area across the entire loading and unloading phases, HLA approaches the classic definition of hysteresis in a more comprehensive way, rather than a difference in pressures at a single time point as expressed through the standard variable CH (Figure 3).

The Corvis STL (Oculus Optikgeräte GmbH, Wetzlar, Germany) is a non-contact tonometer that employs a similar air puff perturbation and has been commercially available since 2011. It employs an ultra high-speed Scheimpflug camera that records the deformation process at 4330 frames/second along an 8 mm horizontal corneal cross-section during corneal deformation.<sup>15,16</sup> Analysis of the images provides insight into the infrared signal behavior observed with the ORA, and because direct analysis of shape is possible, provides additional opportunities for a more direct derivation of biomechanical response.<sup>17,18</sup> Contrary to the ORA, the Corvis STL does not vary the air puff pressure from measurement to measurement. Differences in applied force might confound attempts to directly compare results obtained with these two instruments.<sup>19</sup>

The ORA and Corvis share some limitations. Both measure features of the mechanical response that have not been related directly to corneal elastic modulus or other properties through experimental work. In addition, neither is specifically designed to assess spatial differences in corneal properties across the width and depth of the cornea, and extracorneal structures may have an influence on corneal measurements.<sup>20</sup> The ORA's variable air puff pressure makes it difficult to compare measurements between eyes and across time or interventions.<sup>21,22</sup> Repeatability studies showed that the Corvis can produce reliable measurements of IOP and central corneal thickness (CCT), while the results are more variable when the corneal deformation and biomechanical parameters are analyzed.<sup>19,23–25</sup>

These limitations do not diminish the importance of measuring biomechanical behavior *in vivo*, and both devices have greatly advanced our understanding of corneal biomechanical behavior in many clinically relevant states. Studies that combine tomographic and biomechanical assessment have demonstrated enhanced refractive surgery screening potential<sup>26,27</sup> and suggest that many advances are yet to come in the use of biomechanical measurements for diagnosis and clinical decision making.

### Optical Coherence Elastography (OCE)

Optical coherence tomography (OCT) is a well-established low coherence interferometric imaging technique, providing great resolution and is completely noninvasive.<sup>28,29</sup> In principle, elastography imaging has several ideal elements, such as high-resolution imaging, the application of a mechanical force to cause tissue distortion, re-imaging of the resulting tissue deformation response, and mathematical modeling and analysis to link the observed tissue response to the biomechanical properties of the tissue, e.g. the elastic modulus.

The first OCE investigations of corneal biomechanical properties utilized structural imaging to quantify displacements in the cornea before and after static compression. The heterogeneous elastic properties of the cornea were revealed from the variations in the axial and lateral displacements.<sup>30</sup> This technique was also used to study the changes in normal, edematous, and CXL human corneas in the whole eye-globe configuration at an artificially controlled IOP.<sup>31</sup> The hydration and CXL treatment showed spatially varying results in the ratio of the axial to lateral displacements. Furthermore, the displacement ratio had a greater degree of variance between the treatment conditions when measurements were made in the superior/inferior axis as compared to the nasal/temporal axis, revealing the mechanical anisotropy of the cornea. The technique has evolved, and our group is currently performing clinical studies to evaluate the measurement capabilities of OCE *in vivo* (De Stefano *et al.* In-vivo Assessment of Corneal Biomechanics using Optical Coherence Elastography. ARVO 2017. Baltimore, MD [abstract]). Figure 4 shows an elastogram in the right eye of a healthy 30-year-old male. It is possible to observe the distinct behavior of the anterior and posterior segments of the corneal stroma: even though the compression apparatus is applied to the anterior portion, the posterior stroma has a higher total displacement vector. Another method of noncontact excitation that has been proposed is micro air-pulse stimulation. Unlike the ORA and the Corvis STL, which utilize a relatively long duration and large amplitude air-puff, a short duration ( $\sim 1$  ms) micro air-pulse was used to induce highly-localized displacements, which then propagated as an elastic wave (“rock thrown in a pond”).<sup>32,33</sup> The elastic (or shear) wave is directly related to the elastic modulus, without interference of IOP, thus the technique is able to assess corneal biomechanics in a straightforward fashion.<sup>34,35</sup>

It is important to observe that the techniques described are investigational; thus no device is commercially available yet. However, OCE is a promising method for measuring corneal biomechanical properties in a comprehensive fashion and with high spatial resolution (microns). Moreover, there are some studies describing the use of OCE to assess the biomechanical properties of the crystalline lens, broadening the usage of this technology to other clinical applications in ophthalmology.<sup>36</sup>

## Brillouin Microscopy

Brillouin microscopy is an optical approach to quantification of material properties. In principle, when objects are interrogated with monochromatic light, photons will experience a slight frequency shift that can be related to the material properties of the object and its density.<sup>37</sup> This noninvasive optical technique based on analyzing the Brillouin frequency shift is capable of generating depth-resolved elasticity distribution maps of the cornea and lens with micrometer-scale spatial resolution.<sup>38–40</sup> Brillouin microscopy has been used to investigate the depth-resolved Brillouin shift in human corneal buttons with and without keratoconus,<sup>39</sup> in ex vivo porcine corneas before and after CXL,<sup>40</sup> and in human eyes in vivo.<sup>38</sup> Current limitations include high acquisition time and the system expense, but like OCE, the method is being developed for commercial translation.

## COMPUTATIONAL MODELING

Pertinent goals of computational modeling in corneal imaging include understanding the mechanisms of keratoconus progression, as well as developing an accurate simulation engine for ectasia risk assessment and treatment optimization. One approach to studying complex structures like the cornea is the finite element (FE) method.<sup>41</sup> The cornea and surrounding structures can be represented as a mesh of smaller geometric elements with specified material properties—ideally from patient-specific measurements—and interconnected at element nodes. The response to a simulated structural change is then obtained iteratively from node to node until a solution for the entire structure is obtained (Figure 5). The predictive value of any model depends on the validity of input and assumptions, and progress in high-resolution anterior segment imaging has enabled major gains in our ability to accurately measure corneal geometry for such models.

FE analysis has been used to simulate surgical results in various refractive procedures as well as the biomechanical alterations in keratoconus.<sup>42–45</sup> In a more recent study of three-dimensional modeling of the cornea using patient-specific corneal geometry from Scheimpflug-based tomography, Dupps and Seven performed LASIK and PRK simulations with varied myopic ablation profiles and flap thickness parameters across eyes from LASIK candidates, patients disqualified for LASIK, subjects with atypical topography, and keratoconus subjects in a total of 280 simulations.<sup>46</sup> FE analysis output was then interrogated to extract several risk and outcome variables. Mean maximum principal strain, a variable that express mean strains across the anterior residual stromal bed, was effective at differentiating normal and at-risk eyes in ROC analyses. Strain was highly correlated to thickness-based risk metrics and also predicted large portions of the variance in predicted refractive response to surgery. The accuracy of the same modeling approach was assessed in a 20-eye study of myopic LASIK that demonstrated a mean error of only  $-0.11 \pm 0.34$  D ( $p = 0.2$ ) in predicted outcome, and consideration of patient-specific difference in preoperative CH led to even more accurate predictions.<sup>46</sup>

These are some examples of a growing movement towards using simulation for understanding corneal disease mechanisms and driving rational changes to this approach to treatment. Advances in corneal biomechanical property measurement and patient-specific modeling have the potential to enhance early keratoconus diagnosis, enable personalized,

procedure-specific ectasia risk assessment through simulation and drive optimized treatment design for a variety of corneal refractive conditions.

## CONCLUSIONS

- The relationship between corneal micro- and macro-structure and optical function is at the center of the study of corneal biomechanics.
- Corneal biomechanical features are complex and cannot be fully defined by a single number or expression.
- Commercially available air puff-based corneal biomechanical measurement devices have added greatly to our understanding of corneal responses in health and disease but also have some limitations for distinguishing, by themselves, healthy from suspect corneas. Novel analyses of the corneal responses measured with these devices are an active area of investigation.
- Emerging technologies such as OCT elastography and Brillouin microscopy are promising techniques for spatially resolved corneal biomechanical assessment.
- Computational modeling has the potential to combine information on patient-specific tomography and biomechanics in an approach that may significantly enhance how patients are evaluated before and after corneal refractive procedures.

## Acknowledgments

Support: NIH R01 EY023381; Ohio Third Frontier Innovation Platform Award TECH 13-059; Unrestricted Grant from RPB to the Dept. of Ophthalmology of the Cleveland Clinic Lerner College of Medicine of Case Western Reserve University, NIH-NEI P30 Core Grant (IP30EY025585-01A1), The Pender Ophthalmology Research Fund and the Sara J. Chehel Fund for Ocular Biomechanics Research at the Cole Eye Institute.

## References

1. Seiler T, Matallana M, Sendler S, Bende T. Does Bowman's layer determine the biomechanical properties of the cornea? *Refract Corneal Surg.* 8(2):139–142.
2. Morishige N, Wahlert AJ, Kenney MC, et al. Second-harmonic imaging microscopy of normal human and keratoconus cornea. *Invest Ophthalmol Vis Sci.* 2007; 48(3):1087–1094. DOI: 10.1167/iops.06-1177 [PubMed: 17325150]
3. Jue B, Maurice DM. The mechanical properties of the rabbit and human cornea. *J Biomech.* 1986; 19(10):847–853. DOI: 10.1016/0021-9290(86)90135-1 [PubMed: 3782167]
4. Smolek MK, McCarey BE. Interlamellar adhesive strength in human eyebank corneas. *Investig Ophthalmol Vis Sci.* 1990; 31(6):1087–1095. [PubMed: 2354912]
5. Dupps WJ, Roberts C. Effect of acute biomechanical changes on corneal curvature after photokeratectomy. *J Refract Surg.* 2001; 17(6):658–669. [PubMed: 11758984]
6. Winkler M, Chai D, Kriling S, et al. Nonlinear optical macroscopic assessment of 3-D corneal collagen organization and axial biomechanics. *Investig Ophthalmol Vis Sci.* 2011; 52(12):8818–8827. DOI: 10.1167/iops.11-8070 [PubMed: 22003117]
7. Andreassen TT, Simonsen AH, Oxlund H. Biomechanical properties of keratoconus and normal corneas. *Exp Eye Res.* 1980; 31(4):435–441. [PubMed: 7449878]
8. Randleman JB, Dawson DG, Grossniklaus HE, McCarey BE, Edelhauser HF. Depth-dependent cohesive tensile strength in human donor corneas: implications for refractive surgery. *J Refract Surg.* 2008; 24(1):S85–9. [PubMed: 18269156]

9. Luce DA. Determining in vivo biomechanical properties of the cornea with an ocular response analyzer. *J Cataract Refract Surg.* 2005; 31(1):156–162. DOI: 10.1016/j.jcrs.2004.10.044 [PubMed: 15721708]
10. Fontes BM, Ambrósio R, Jardim D, Velarde GC, Nosé W. Corneal Biomechanical Metrics and Anterior Segment Parameters in Mild Keratoconus. *Ophthalmology.* 2010; 117(4):673–679. DOI: 10.1016/j.ophtha.2009.09.023 [PubMed: 20138369]
11. Shah S, Laiquzzaman M, Bhojwani R, Mantry S, Cunliffe I. Assessment of the biomechanical properties of the cornea with the ocular response analyzer in normal and keratoconic eyes. *Investig Ophthalmol Vis Sci.* 2007; 48(7):3026–3031. DOI: 10.1167/iovs.04-0694 [PubMed: 17591868]
12. Goldich Y, Marcovich AL, Barkana Y, et al. Clinical and corneal biomechanical changes after collagen cross-linking with riboflavin and UV irradiation in patients with progressive keratoconus: results after 2 years of follow-up. *Cornea.* 2012; 31(6):609–614. DOI: 10.1097/ICO.0b013e318226bf4a [PubMed: 22378112]
13. Hallahan KM, Sinha Roy A, Ambrosio R, Salomao M, Dupps WJ. Discriminant value of custom ocular response analyzer waveform derivatives in keratoconus. *Ophthalmology.* 2014; 121(2):459–468. DOI: 10.1016/j.ophtha.2013.09.013 [PubMed: 24289916]
14. Hallahan KM, Rocha K, Roy AS, Randleman JB, Stulting RD, Dupps WJ. Effects of corneal cross-linking on ocular response analyzer waveform-derived variables in keratoconus and postrefractive surgery ectasia. *Eye Contact Lens.* 2014; 40(6):339–344. DOI: 10.1097/ICL.0000000000000090 [PubMed: 25365551]
15. Koproński R, Ambrósio R, Reisdorf S. Scheimpflug camera in the quantitative assessment of reproducibility of high-speed corneal deformation during intraocular pressure measurement. *J Biophotonics.* 2015; 8(11–12):968–978. DOI: 10.1002/jbio.201400137 [PubMed: 25623926]
16. Lee R, Chang RT, Wong IYH, Lai JSM, Lee JWY, Singh K. Novel Parameter of Corneal Biomechanics That Differentiate Normals From Glaucoma. *J Glaucoma.* 2016; 25(6):e603–e609. DOI: 10.1097/IJG.0000000000000284 [PubMed: 26035421]
17. Hashemi H, Asgari S, Mortazavi M, Ghaffari R. Evaluation of Corneal Biomechanics After Excimer Laser Corneal Refractive Surgery in High Myopic Patients Using Dynamic Scheimpflug Technology. *Eye Contact Lens.* 2016; 0(0):1–7. DOI: 10.1097/ICL.0000000000000280
18. Salvetat ML, Zeppieri M, Tosoni C, Felletti M, Grasso L, Brusini P. Corneal Deformation Parameters Provided by the Corvis-ST Pachy-Tonometer in Healthy Subjects and Glaucoma Patients. *J Glaucoma.* 2015; 24(8):568–574. DOI: 10.1097/IJG.0000000000000133 [PubMed: 25318572]
19. Lanza M, Iaccarino S, Bifani M. In vivo human corneal deformation analysis with a Scheimpflug camera, a critical review. *J Biophotonics.* 2016; 9(5):464–477. DOI: 10.1002/jbio.201500233 [PubMed: 26871552]
20. Kling S, Marcos S, BS, et al. Contributing Factors to Corneal Deformation in Air Puff Measurements. *Investig Ophthalmology Vis Sci.* 2013; 54(7):5078–5085. DOI: 10.1167/iovs.13-12509
21. Roberts CJ. Concepts and misconceptions in corneal biomechanics. *J Cataract Refract Surg.* 2014; 40(6):862–869. DOI: 10.1016/j.jcrs.2014.04.019 [PubMed: 24857435]
22. Roberts CJ. Importance of accurately assessing biomechanics of the cornea. *Curr Opin Ophthalmol.* 2016; 27(4):285–291. DOI: 10.1097/ICU.0000000000000282 [PubMed: 27152485]
23. Nemeth G, Hassan Z, Csutak A, Szalai E, Berta A, Modis L. Repeatability of Ocular Biomechanical Data Measurements With a Scheimpflug-Based Noncontact Device on Normal Corneas. *J Refract Surg.* 2013; 29(8):558–563. DOI: 10.3928/1081597X-20130719-06 [PubMed: 23909783]
24. Bak-Nielsen S, Pedersen IB, Ivarsen A, Hjortdal J. Repeatability, Reproducibility, and Age Dependency of Dynamic Scheimpflug-Based Pneumotonometer and Its Correlation With a Dynamic Bidirectional Pneumotometry Device. *Cornea.* 2015; 34(1):71–77. DOI: 10.1097/ICO.0000000000000293 [PubMed: 25393092]
25. Bak-Nielsen S, Pedersen IB, Ivarsen A, Hjortdal J. Dynamic Scheimpflug-based assessment of keratoconus and the effects of corneal cross-linking. *J Refract Surg.* 2014; 30(6):408–414. DOI: 10.3928/1081597X-20140513-02 [PubMed: 24972407]



26. Luz A, Lopes B, Hallahan KM, et al. Discriminant Value of Custom Ocular Response Analyzer Waveform Derivatives in Forme Fruste Keratoconus. *Am J Ophthalmol.* 2016; 164:14–21. DOI: 10.1016/j.ajo.2015.12.020 [PubMed: 26743618]
27. Vinciguerra R, Elsheikh A, Roberts CJ, et al. Influence of Pachymetry and Intraocular Pressure on Dynamic Corneal Response Parameters in Healthy Patients. *J Refract Surg.* 2016; 32(8):550–561. DOI: 10.3928/1081597X-20160524-01 [PubMed: 27505316]
28. Ophir J, Cespedes I, Ponnekanti H, Yazdi Y, Li X. Elastography: A Quantitative Method for Imaging the Elasticity of Biological Tissues. *Ultrason Imaging.* 1991; 13(2):111–134. DOI: 10.1177/016173469101300201 [PubMed: 1858217]
29. Schmitt J. OCT elastography: imaging microscopic deformation and strain of tissue. *Opt Express.* 1998; 3(6):199. doi: 10.1364/OE.3.000199 [PubMed: 19384362]
30. Ford MR, Dupps WJ, Rollins AM, Roy AS, Hu Z. Method for optical coherence elastography of the cornea. *J Biomed Opt.* 2011; 16(1):16005. doi: 10.1117/1.3526701
31. Ford MR, Roy AS, Rollins AM, Dupps WJ. Serial biomechanical comparison of edematous, normal, and collagen crosslinked human donor corneas using optical coherence elastography. *J Cataract Refract Surg.* 2014; 40(6):1041–1047. DOI: 10.1016/j.jcrs.2014.03.017 [PubMed: 24767794]
32. Wang S, Larin KV, Li J, et al. A focused air-pulse system for optical-coherence-tomography-based measurements of tissue elasticity. *Laser Phys Lett.* 2013; 10(7):75605. doi: 10.1088/1612-2011/10/7/075605
33. Wang S, Larin KV. Shear wave imaging optical coherence tomography (SWI-OCT) for ocular tissue biomechanics. *Opt Lett.* 2014; 39(1):41–44. [PubMed: 24365817]
34. Singh M, Li J, Han Z, et al. Investigating Elastic Anisotropy of the Porcine Cornea as a Function of Intraocular Pressure With Optical Coherence Elastography. *J Refract Surg.* 2016; 32(8):562–567. DOI: 10.3928/1081597X-20160520-01 [PubMed: 27505317]
35. Singh M, Li J, Vantipalli S, Han Z, Larin KV, Twa MD. Optical coherence elastography for evaluating customized riboflavin/UV-A corneal collagen crosslinking. *J Biomed Opt.* 2017; 22(9):91504. doi: 10.1117/1.JBO.22.9.091504 [PubMed: 28055060]
36. Wu C, Han Z, Wang S, et al. Assessing Age-Related Changes in the Biomechanical Properties of Rabbit Lens Using a Coaligned Ultrasound and Optical Coherence Elastography System. *Invest Ophthalmol Vis Sci.* 2015; 56(2):1292–1300. DOI: 10.1167/iovs.14-15654 [PubMed: 25613945]
37. Scarcelli G, Yun SH. Confocal Brillouin microscopy for three-dimensional mechanical imaging. *Nat Photonics.* 2007; 2:39–43. DOI: 10.1038/nphoton.2007.250 [PubMed: 19812712]
38. Scarcelli G, Yun SH. In vivo Brillouin optical microscopy of the human eye. *Opt Express.* 2012; 20(8):9197. doi: 10.1364/OE.20.009197 [PubMed: 22513631]
39. Scarcelli G, Besner S, Pineda R, Yun SH. Biomechanical Characterization of Keratoconus Corneas Ex Vivo With Brillouin Microscopy. *Investig Ophthalmology Vis Sci.* 2014; 55(7):4490. doi: 10.1167/iovs.14-14450
40. Scarcelli G, Kling S, Quijano E, Pineda R, Marcos S, Yun SH. Brillouin microscopy of collagen crosslinking: noncontact depth-dependent analysis of corneal elastic modulus. *Invest Ophthalmol Vis Sci.* 2013; 54(2):1418–1425. DOI: 10.1167/iovs.12-11387 [PubMed: 23361513]
41. Woo S-Y, Kobayashi AS, Schlegel WA, Lawrence C. Nonlinear material properties of intact cornea and sclera. *Exp Eye Res.* 1972; 14(1):29–39. DOI: 10.1016/0014-4835(72)90139-X [PubMed: 5039845]
42. Sinha Roy A, Dupps WJ, Roberts CJ. Comparison of biomechanical effects of small-incision lenticule extraction and laser in situ keratomileusis: finite-element analysis. *J Cataract Refract Surg.* 2014; 40(6):971–980. DOI: 10.1016/j.jcrs.2013.08.065 [PubMed: 24857440]
43. Sinha Roy A, Dupps WJ. Effects of altered corneal stiffness on native and postoperative LASIK corneal biomechanical behavior: A whole-eye finite element analysis. *J Refract Surg.* 2009; 25(10):875–887. DOI: 10.3928/1081597X-20090917-09 [PubMed: 19835328]
44. Seven I, Sinha Roy A, Dupps WJ. Patterned corneal collagen crosslinking for astigmatism: Computational modeling study. *J Cataract Refract Surg.* 2014; 40(6):943–953. DOI: 10.1016/j.jcrs.2014.03.019 [PubMed: 24767795]

45. Carvalho LA, Prado M, Cunha RH, et al. Keratoconus prediction using a finite element model of the cornea with local biomechanical properties. *Arq Bras Oftalmol.* 2009; 72(2):139–145. DOI: 10.1590/S0004-27492009000200002 [PubMed: 19466318]
46. Seven I, Vahdati A, De Stefano VS, Krueger RR, D William J Jr. Comparison of Patient-Specific Computational Modeling Predictions and Clinical Outcomes of LASIK for Myopia. *Investig Ophthalmology Vis Sci.* 2016; 57(14):6287–6297. DOI: 10.1167/iovs.16-19948

Author Manuscript

Author Manuscript

Author Manuscript

Author Manuscript

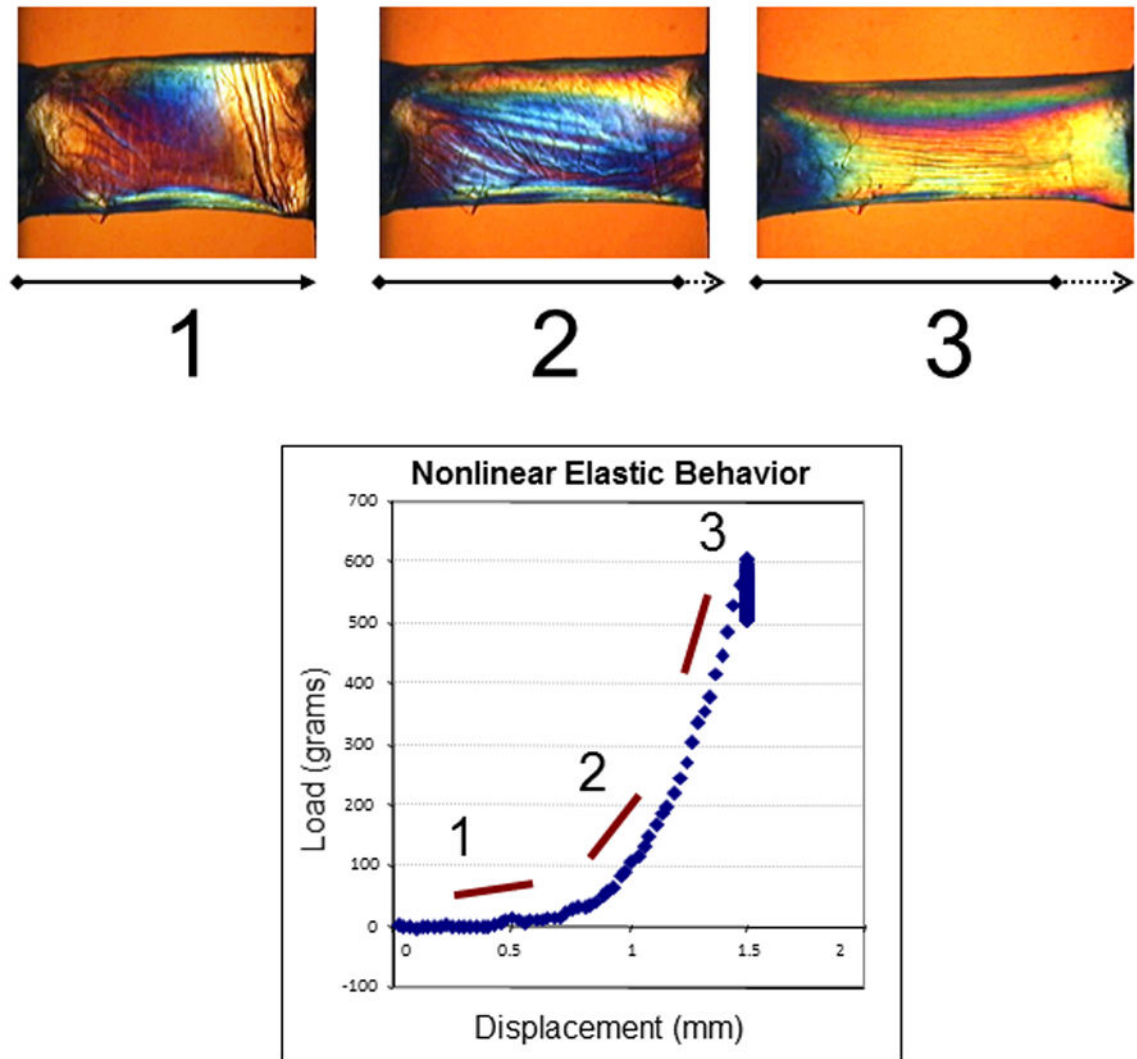


**Figure 1.** Experiment illustrating the nonlinear elastic properties of a 7 mm, full-thickness horizontal corneal strip from a 63-year-old donor. Progressive stretching of the sample (1, 2 and 3) and measurement of the induced load (stress) allows calculation of the elastic (Young's) modulus from the slope of the stress-strain relationship.

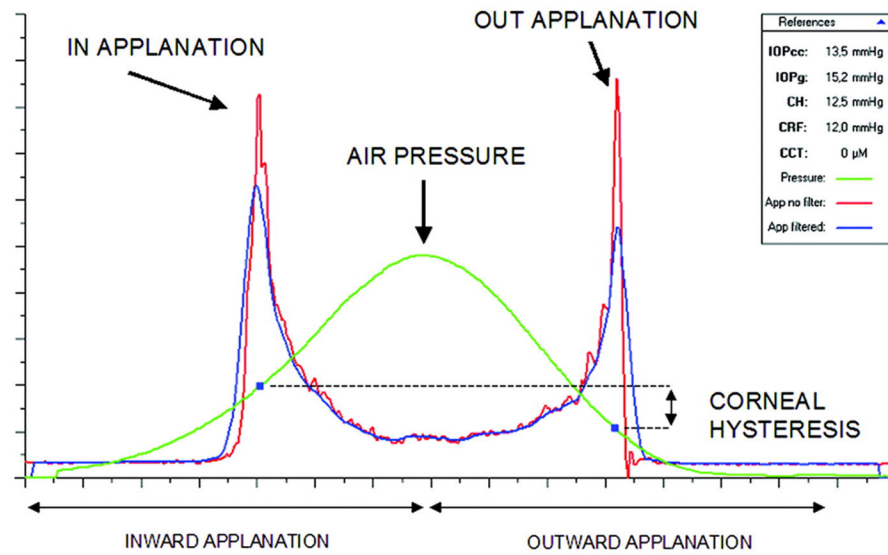


**Figure 2.** Example of a graph obtained from the Ocular Response Analyzer. Both applanation events are indicated in the infrared signal reflection peaks measured by the device. The pressure values in those peaks, P1 and P2, are used to calculate the corneal hysteresis variable (CH).

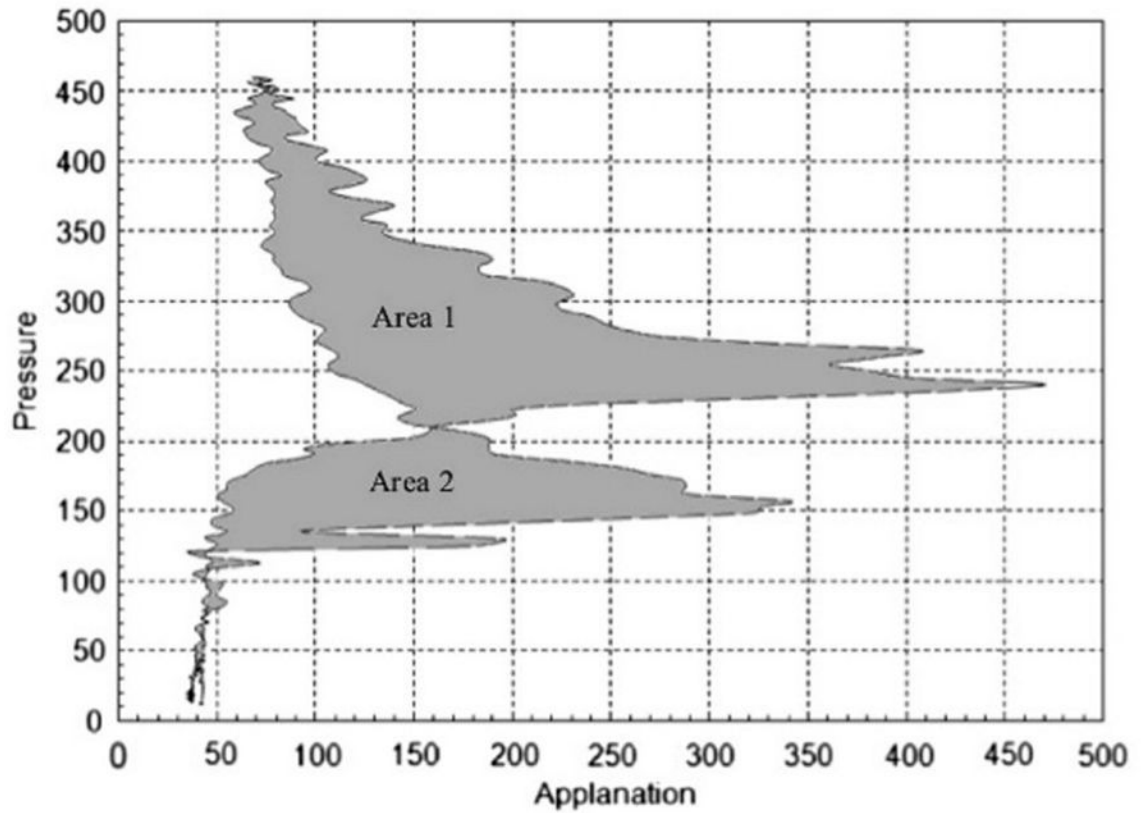


**Figure 3.** Calculation of hysteresis loop area (HLA). From each measurement by the ORA, pressure values of the signal output were plotted against applanation values at each time point. HLA represents the sum of areas 1 and 2 within the closed loop. Adapted from Hallahan KM *et al.* Discriminant Value of Custom Ocular Response Analyzer Waveform Derivatives in Keratoconus. *Ophthalmology*. 2014;121:459–468.

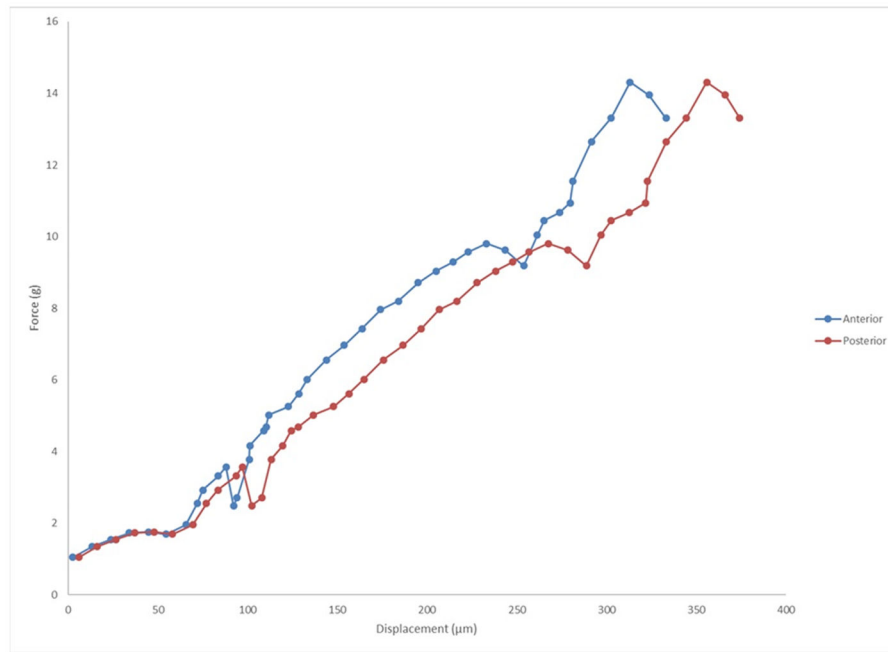


**Figure 4.** Graph of force vs. displacement after optical coherence elastography (OCE) assessment *in vivo* in a normal cornea. One can observe that with the same amount of stress applied to the cornea, the anterior and posterior segments of the tissue behave distinctly.

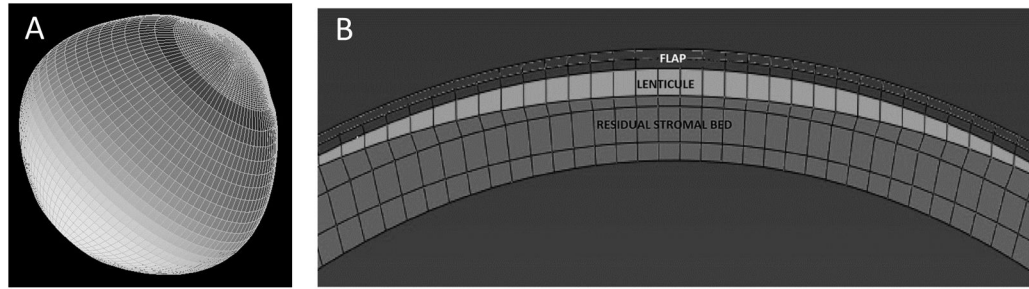


**Figure 5.**

A: an example of a corneoscleral mesh. B: defined regions within the mesh for simulation of myopic photoablative surgery, including flap, lenticule (area to be ablated) and the residual stromal bed.